MODELING AND SIMULATION OF IN-SITU COMBUSTION OF OIL SHALE AS ENHANCED OIL RECOVERY TECHNIQUE IN POROUS MEDIA

OYUBU, J. P., OLAYIWOLA, R. O., YAHAYA, Y. A., & COLE, A. T.
Department of Mathematics,
Federal University of Technology, Minna, Nigeria.
E-mail: oyubuj@yahoo.com **Phone No**: +234-806-342-2423

Abstract
Oil shale is fast becoming an important alternative energy source due to its huge reserves. With oil shale it is quite possible to satisfy the future oil requirement. This study presents a one-dimensional transient coupled mass and heat transport model incorporating combustion front velocity, describing the in-situ combustion of oil shale in a porous medium. The coupled nonlinear partial differential equations describing the phenomenon were decoupled using perturbation method and solved analytically using eigenfunctions expansion technique and direct integration. The governing parameters of the problem are the Frank-Kamenetskii number (δ), Peclet energy number (P_e), Peclet mass number (P_{em}), Reynolds number (R_e), Darcy number (D_a) and Heat exchange coefficient (σ). The results obtained were presented graphically and discussed. These results showed that the species concentrations (X and Y) and temperatures (θ and ϕ) distribution in porous medium are significantly influenced by the Frank-Kamenetskii number, heat exchange coefficient, time and distance.

Keywords: Combustion, In-situ, Oil shale, Porous medium, Stimulation.

Introduction
Oil shale is currently gaining attention as a potential abundant source of oil whenever the price of crude oil rises. Oil shale is found all over the world, including China, Israel, and Russia. The United States, however, has the most shale resources. The oil shale in its natural state contains kerogen, a precursor to petroleum. Kerogen is the solid, insoluble, organic material in the shale that can be converted to oil and other petroleum products by pyrolysis and distillation. However, all the types of kerogen consist mainly of hydrocarbons; smaller amounts of sulphur, oxygen and nitrogen; and a variety of minerals (Abdelrahman, 2015).

Deposits of oil shale have been found in 27 countries worldwide and this is becoming an important alternative energy source due to its huge reserves. With oil shale, it is quite possible to satisfy the future oil requirement. Upon being heated, kerogen in oil shale can be converted to oil and gas. The heating process is called pyrolysis or retorting (Zheng et al., 2017).

Several works have been done on the in-situ combustion of oil shale. Lapene *et al.* (2007) modeled coupled mass and heat transport in reactive porous medium using homogeneous description at a Darcy-scale. Local non-equilibrium transport of heat was treated with a two field temperature, one for the gas and one for the solid phase.

Olayiwola *et al.* (2011) extended Lapene *et al.* (2007) work to a situation where there is Arrhenius heat generation and chemical reaction. They made additional assumption that the reaction is in steady-state so that time derivatives are zero $\left(\frac{\partial}{\partial t}=0\right)$. They examined the properties of solution of the model and obtained the analytical solution using asymptotic expansion.

In another study, Olayiwola (2012) studied coupled heat transport in Arrhenius reactive porous medium using a homogeneous description at the Darcy-scale. In this study, it was assumed that there is a perfect contact between gas and solid phase. Eigenfunctions expansion technique was used and the results showed that the heat transfer increases as Frank-Kamenetskii number increases and scaled thermal conductivity decreases.

Zheng et al. (2017) focused on the numerical simulation of in-situ combustion of oil shale. Numerical test was used for the stimulation of oil shale and their result showed that varying gas injection rate and oxygen was important in the field test in-situ combustion.

It is interesting to note that this study extends the work of Olayiwola (2012) by incorporating combustion front velocity, continuity and momentum equations and assume no perfect contact between gas and solid phases.

Model Formulation
The partial differential equations that describe the in-situ combustion of oil shale can be written as (Olayiwola, 2012):
The continuity equation:

$$\frac{\partial \rho}{\partial t} + \frac{\partial (\rho u_c)}{\partial x} = 0 \tag{1}$$

The momentum equation:

$$\rho\left(\frac{\partial u_c}{\partial t} + u_c \frac{\partial u_c}{\partial x}\right) = -\frac{\partial p}{\partial x} + \frac{\partial}{\partial x}\left(\mu \frac{\partial u_c}{\partial x}\right) \tag{2}$$

The gas phase energy equation:

$$\left.\begin{aligned}
\rho_g \varepsilon c_g \left(\frac{\partial T_g}{\partial t} - u_c \frac{\partial T_g}{\partial x}\right) + \rho_g \varepsilon c_g u_f \frac{\partial T_g}{\partial x} = \frac{\partial}{\partial x}\left(\kappa_g \frac{\partial T_g}{\partial x}\right) + \Gamma\left(T_g - T_s\right) + h\left(T_e - T_g\right) \\
+ \varepsilon \Delta H A\, C_f^\alpha C_{ox}^\beta e^{-\frac{E}{RT_s}}
\end{aligned}\right\} \tag{3}$$

The solid phase energy equation:

$$\rho_s (1-\varepsilon)c_s\left(\frac{\partial T_s}{\partial t} - u_c \frac{\partial T_s}{\partial x}\right) = \frac{\partial}{\partial x}\left(\kappa_s \frac{\partial T_s}{\partial x}\right) - \Gamma\left(T_g - T_s\right) + h\left(T_e - T_s\right) + (1-\varepsilon)\Delta H A C_f^\alpha C_{ox}^\beta e^{-\frac{E}{RT_s}} \tag{4}$$

The oxygen mass balance:

$$\varepsilon\rho_g\left(\frac{\partial C_{ox}}{\partial t} - u_c \frac{\partial C_{ox}}{\partial x}\right) + \varepsilon\rho_g u_f \frac{\partial C_{ox}}{\partial x} = \rho_g \varepsilon \frac{\partial}{\partial x}\left(D_{ox}\frac{\partial C_{ox}}{\partial x}\right) + \varepsilon A C_f^\alpha C_{ox}^\beta e^{-\frac{E}{RT_s}} \tag{5}$$

The fuel mass balance:

$$(1-\varepsilon)\rho_g\left(\frac{\partial C_f}{\partial t} - u_c \frac{\partial C_f}{\partial x}\right) = (1-\varepsilon)A C_f^\alpha C_{ox}^\beta e^{-\frac{E}{RT_s}} \tag{6}$$

Darcy's law

$$u_f = -\frac{K}{\mu}\left(\frac{\partial P}{\partial x} - \rho_g \nabla Z\right) \tag{7}$$

where E is the activation energy, Z is the frequency factor, α and β are orders of the gaseous reaction, ρ_g is gas density, R is the gas constant, u_c is combustion front velocity, κ_s is thermal conductivity of solid phase, κ_g is thermal conductivity of gas phase, μ is viscosity, t is time, x is position, ε is the porosity, c_s is heat capacity of solid phase, c_g is the heat capacity of gas phase, T_e is the external temperature, T_s is the temperature of solid phase, T_g is the temperature of gas phase, ΔH is heat generation constant, h is heat transfer coefficient, C_m is concentration of oxygen, C_f is fuel concentration, Γ is exchange term between the phases, K is the permeability , D_{ox} is the diffusion of oxygen, u_f is filtration velocity and P is the pressure.

The dependence of thermal conductivities, dynamic viscosity and oxygen diffusion coefficient on the temperatures is taken into account by mathematical expression (Olayiwola, 2012):

$$k_g = k_{g0}\left(\frac{T_g}{T_0}\right), \quad k_s = k_{s0}\left(\frac{T_s}{T_0}\right), \quad \mu = \mu_0\left(\frac{T_s}{T_0}\right), \quad D_{ox} = D_0\left(\frac{T_g}{T_0}\right) \tag{8}$$

where k_{s0} the initial solid phase thermal conductivity, k_{g0} is the initial gas phase thermal conductivity T_0 is the initial temperature of the medium, μ_0 is the initial viscosity, D_0 is the initial diffusion coefficient, D_{0z} is the diffusion of oxygen, k_s is the thermal conductivity of the solid phase, k_g is the thermal conductivity of the gas phase and μ is the viscosity.

Coordinate Transformation

Here, we shall neglect the gravitational effect due to the small size in the vertical direction and we let $\rho_g = \rho_s = \rho$. It simple to eliminate the continuity equation (1) by means of streamline function (Olayiwola, 2011):

$$\eta(x,t) = \left(\rho^2\right)^{\frac{1}{2}}\int_0^x \rho(s,t)\,ds \tag{9}$$

Then, the coordinate transformation becomes:

$$\frac{\partial}{\partial x} \rightarrow \frac{\partial}{\partial \eta}\frac{\partial \eta}{\partial x} = \frac{\partial}{\partial \eta} \tag{10}$$

$$\frac{\partial}{\partial t} \rightarrow \frac{\partial}{\partial \eta}\frac{\partial \eta}{\partial t} + \frac{\partial}{\partial t} = -u_c\frac{\partial}{\partial \eta} + \frac{\partial}{\partial t} \tag{11}$$

Using equations (10) and (11), equations (1) – (8) can be simplified to:

$$\frac{\partial u_c}{\partial t} = -\frac{1}{\rho}\frac{\partial P}{\partial \eta} + \frac{\mu_0}{\rho T_0}\frac{\partial}{\partial \eta}\left(T_s\frac{\partial u_c}{\partial \eta}\right) \tag{12}$$

$$\left.\begin{aligned}
\left(\frac{\partial T_g}{\partial t}-2u_c\frac{\partial T_g}{\partial \eta}\right)+u_f\frac{\partial T_g}{\partial \eta}&=\frac{k_{g0}}{\rho\varepsilon c_g T_0}\frac{\partial}{\partial \eta}\left(T_g\frac{\partial T_g}{\partial \eta}\right)+\frac{\Gamma}{\rho\varepsilon c_g}\left(T_g-T_s\right)+\frac{h}{\rho\varepsilon c_g}\left(T_e-T_g\right)+\\
\frac{\Delta HA}{\rho c_g}C_f^\alpha C_{ox}^\beta e^{-\frac{E}{RT_s}}&
\end{aligned}\right\} \quad (13)$$

$$\left.\begin{aligned}
\left(\frac{\partial T_s}{\partial t}-2u_c\frac{\partial T_s}{\partial \eta}\right)&=\frac{k_{s0}}{\rho(1-\varepsilon)c_s T_0}\frac{\partial}{\partial \eta}\left(T_s\frac{\partial T_s}{\partial \eta}\right)-\frac{\Gamma}{\rho(1-\varepsilon)c_s}\left(T_g-T_s\right)+\frac{h}{\rho(1-\varepsilon)c_s}\left(T_e-T_s\right)+\\
\frac{\Delta HA}{\rho c_s}C_f^\alpha C_{ox}^\beta e^{-\frac{E}{RT_s}}&
\end{aligned}\right\} \quad (14)$$

$$\left(\frac{\partial C_{ox}}{\partial t}-2u_c\frac{\partial C_{ox}}{\partial \eta}\right)+u_f\frac{\partial C_{ox}}{\partial \eta}=\frac{D_0}{T_0}\frac{\partial}{\partial \eta}\left(T_g\frac{\partial C_{ox}}{\partial \eta}\right)+\frac{A}{\rho}C_f^\alpha C_{ox}^\beta e^{-\frac{E}{RT_s}} \quad (15)$$

$$\left(\frac{\partial C_f}{\partial t}-2u_c\frac{\partial C_f}{\partial \eta}\right)=\frac{A}{\rho}C_f^\alpha C_{ox}^\beta e^{-\frac{E}{RT_s}} \quad (16)$$

$$\frac{\partial P}{\partial \eta}=-\frac{\mu}{K}u_f \quad (17)$$

Assuming the porous space of the medium is filled initially with fuel and oxygen. Then, the initial and boundary conditions are given as follows:

Initial conditions:
At $t=0$ and $\forall \eta$, $u_c=u_{inj}$, $T_g=T_0$, $T_s=T_0$, $C_{ox}=0$, $C_f=C_{f0}$ $\qquad$ (18)

Boundary conditions:

$$\left.\begin{aligned}
\frac{\partial T_s}{\partial \eta}\bigg|_{\eta=0}&=0, \qquad \frac{\partial T_s}{\partial \eta}\bigg|_{\eta=L}=0\\[4pt]
T_g\bigg|_{\eta=0}&=T_{inj}, \qquad \frac{\partial T_g}{\partial \eta}\bigg|_{\eta=L}=0\\[4pt]
C_{ox}\bigg|_{\eta=0}&=C_{ox0}, \qquad \frac{\partial C_{ox}}{\partial \eta}\bigg|_{\eta=L}=0\\[4pt]
u_c\bigg|_{\eta=0}&=u_{inj}, \qquad u_c\bigg|_{\eta=L}=0\\[4pt]
C_f\bigg|_{\eta=0}&=C_{f0}\\[4pt]
P\bigg|_{\eta=L}&=P_{outlet}
\end{aligned}\right\} \quad (19)$$

Method of Solution

In order to solve the in-situ combustion problem modeled by equations (12) – (19), we consider the pressure gradient to be parabolic (Olayiwola, 2012)

$$\frac{\partial p}{\partial \eta}=\eta(1-\eta) \quad (20)$$

Non-dimensionalisation

We non-dimensionalised (15) - (22) using the following set of dimensionless variables:

$$\theta = \frac{E}{RT^2{}_0}(T_s - T_0), \quad \phi = \frac{E}{RT_0{}^2}(T_g - T_0) \quad \in = \frac{RT_0}{E}, \quad \eta' = \frac{\eta}{L}, \quad t' = \frac{u_{inj}t}{L}$$

$$X = \frac{C_{ax}}{C_{ax0}}, \quad Y = \frac{C_f}{C_{f0}}, \quad u = \frac{u_C}{u_{inj}}, \quad v = \frac{u_f}{u_{inj}}, \quad P' = \frac{P}{\rho u_{inj}^2},$$

$$(21)$$

to obtain (after dropping the primes)

$$\frac{\partial u}{\partial t} = -\frac{\partial P}{\partial \eta} + \frac{1}{Re}\frac{\partial}{\partial \eta}\left((1+\in\theta)\frac{\partial u}{\partial \eta}\right) \tag{22}$$

$$\frac{\partial \phi}{\partial t} - 2u\frac{\partial \phi}{\partial \eta} + v\frac{\partial \phi}{\partial \eta} = \frac{1}{Pe}\frac{\partial}{\partial \eta}\left((1+\in\phi)\frac{\partial \phi}{\partial \eta}\right) + \sigma(\phi - \theta) + \gamma(a - \phi) + \delta\, Y^\alpha X^\beta e^{\frac{\theta}{1+\in\theta}} \tag{23}$$

$$\frac{\partial \theta}{\partial t} - 2u\frac{\partial \theta}{\partial \eta} = \frac{1}{Pe}\frac{\partial}{\partial \eta}\left((1+\in\theta)\frac{\partial \theta}{\partial \eta}\right) - \sigma_1(\phi - \theta) + \gamma_1(a_1 - \phi) + \delta_1 Y^\alpha X^\beta e^{\frac{\theta}{1+\in\theta}} \tag{24}$$

$$\frac{\partial X}{\partial t} - 2u\frac{\partial X}{\partial \eta} + v\frac{\partial X}{\partial \eta} = \frac{1}{Pem}\frac{\partial}{\partial \eta}\left((1+\in\phi)\frac{\partial X}{\partial \eta}\right) + \delta_2 Y^\alpha X^\beta e^{\frac{\theta}{1+\in\theta}} \tag{25}$$

$$\frac{\partial Y}{\partial t} - 2u\frac{\partial Y}{\partial \eta} = \delta_3 Y^\alpha X^\beta e^{\frac{\theta}{1+\in\theta}} \tag{26}$$

$$v = Da\, Re\frac{\partial p}{\partial \eta} \tag{27}$$

$$\phi(\eta,0)=0, \quad \phi(0,t)=q, \quad \left.\frac{\partial \phi}{\partial \eta}\right|_{\eta=1}=0$$

$$\theta(\eta,0)=0, \quad \theta(0,t)=q_2 \quad \left.\frac{\partial \theta}{\partial \eta}\right|_{\eta=1}=0,$$

$$X(\eta,0)=0, \quad X(0,t)=1, \quad \left.\frac{\partial X}{\partial \eta}\right|_{\eta=1}=0 \tag{28}$$

$$Y(\eta,0)=1, \quad Y(0,t)=1$$

$$\left.P\right|_{\eta=1}=q_1$$

$$u(\eta,0)=1, \quad \left.u\right|_{\eta=0}=1, \quad \left.u\right|_{\eta=1}=0$$

where

$$R_e = \frac{\rho L u_{inj}}{\mu_0} = \frac{L u_{inj}}{\upsilon} = \text{Reynolds number}, \quad P_e = \frac{\rho \varepsilon c_g L u_{inj}}{\kappa_{g0}} = \text{Peclet number}, \quad P_{em} = \frac{L u_{inj}}{D_1} =$$

Mass transfer peclet number, $\sigma = \dfrac{\Gamma L}{\rho \varepsilon c_g u_{inj}} = $ Heat exchange coefficient, $\sigma_1 = \dfrac{\Gamma L}{\rho \varepsilon c_g u_{inj}} =$

Heat exchange coefficient, $\gamma_1 = \dfrac{hL}{\rho \varepsilon c_g u_{inj}}$, $\delta_1 = \dfrac{L \Delta HA}{\rho c_g \in T_0 u_{inj}} e^{-\frac{E}{RT_0}} = $ Frank-kameneskii

parameter, $a_1 = \dfrac{T_e - T_0}{\in T_0}$, $\delta_2 = \dfrac{LAC_{f0}^{\alpha} C_{ox0}^{\beta-1}}{\rho u_{inj}} e^{-\frac{E}{RT_0}}$, $\delta_3 = \dfrac{LAC_{f0}^{\alpha-1} C_{ox0}^{\beta}}{\rho u_{inj}} e^{-\frac{E}{RT_0}}$, $D_a = \dfrac{K}{L^2} = $ Darcy

number,

$\gamma = \dfrac{hL}{\rho \varepsilon c_g u_{inj}}$, $\delta = \dfrac{L \Delta HA}{\rho c_g \in T_0 u_{inj}} e^{-\frac{E}{RT_0}} = $ Frank-kameneskii parameter, $a = \dfrac{T_e - T_0}{\in T_0}$, $b = \dfrac{c_s \in T_0}{\Delta H}$

$P_{em} = \dfrac{L u_{inj}}{D_1} = $ Mass transfer peclet number, $c = \dfrac{c_g \in T_0}{\Delta H}$, $d = \dfrac{c_g T_0}{\Delta H}$

Solution by Eigenfunctions Expansion Method

Here, equations (22) - (28) is solve using eigenfunctions expansion method. In the limit of $\epsilon \to 0$, Ayeni (1978) has shown that e^{θ_0} can be approximated as $1 + (e-2)\theta_0$. Suppose the solution u, θ, ϕ, X and Y in equations (22) – (28) can be expressed as:

$$\left.\begin{array}{l} u = \in u_0 + \in^2 u_1 + ... \\ \theta = \theta_0 + \in \theta_1 + ... \\ \phi = \phi_0 + \in \phi_1 + ... \\ X = X_0 + \in X_1 + ... \\ Y = Y_0 + \in Y_1 + ... \end{array}\right\} \qquad (29)$$

and let

$$\left.\begin{array}{l} D_a = p \in, \sigma = f \in \\ \delta = g \in, \sigma_1 = h \in \\ \delta_1 = j \in, \delta_2 = m \in \end{array}\right\} \qquad (30)$$

Substituting (29) and (30) into (22) – (28) and obtain the order of $\in$ as follows:

$$\frac{\partial \phi_0}{\partial t} = \frac{1}{Pe} \frac{\partial^2 \phi_0}{\partial \eta^2} + \gamma (a - \phi_0) \qquad \phi_0(\eta,0)=0, \qquad \phi_0(0,t)=q, \qquad \left.\frac{\partial \phi_0}{\partial \eta}\right|_{\eta=1} = 0 \qquad (31)$$

$$\frac{\partial \theta_0}{\partial t} = \frac{1}{Pe} \frac{\partial^2 \theta_0}{\partial \eta^2} + \gamma_1 (a_1 - \theta_0) \qquad \theta_0(\eta,0)=0, \qquad \phi_0(0,t)=q_2, \qquad \left.\frac{\partial \theta_0}{\partial \eta}\right|_{\eta=1} = 0 \qquad (32)$$

$$\frac{\partial X_0}{\partial t} = \frac{1}{Pem} \frac{\partial^2 X_0}{\partial \eta^2}, \qquad X_0(\eta,0)=0, \qquad X_0(0,t)=1, \qquad \left.\frac{\partial X_0}{\partial \eta}\right|_{\eta=1} = 0 \qquad (33)$$

$$\frac{\partial Y_0}{\partial t} = 0, \qquad Y_0(\eta,0)=1, \qquad Y_0(0,t)=1 \qquad (34)$$

$$\frac{\partial u_0}{\partial t} = \frac{1}{Re}\frac{\partial^2 u_0}{\partial \eta^2}, \qquad u_0(\eta,0)=\frac{1}{\epsilon}, \qquad u_0(0,t)=\frac{1}{\epsilon}, \qquad u_0(1,t)=0 \tag{35}$$

$$\left.\begin{aligned}
\frac{\partial \phi_1}{\partial t} &= \frac{1}{Pe}\frac{\partial^2 \phi_1}{\partial \eta^2} + \frac{1}{Pe}\phi_0\frac{\partial^2 \phi_0}{\partial \eta^2} + \frac{1}{Pe}\left(\frac{\partial \phi_0}{\partial \eta}\right)^2 + 2u_0\frac{\partial \phi_0}{\partial \eta} + p\,Re\eta(1-\eta)\frac{\partial \phi_0}{\partial \eta} + f(\phi_0-\theta_0) \\
&\quad -\gamma\phi_1 + gY_0^\alpha X_0^\beta (1+(e-2)\wp_0), \qquad \phi_1(\eta,0)=0, \qquad \phi_1(0,t)=0, \qquad \left.\frac{\partial \phi_1}{\partial \eta}\right|_{\eta=1}=0
\end{aligned}\right\} \tag{36}$$

$$\left.\begin{aligned}
\frac{\partial \theta_1}{\partial t} &= \frac{1}{Pe}\frac{\partial^2 \theta_1}{\partial \eta^2} + \frac{1}{Pe}\theta_0\frac{\partial^2 \theta_0}{\partial \eta^2} + \frac{1}{Pe}\left(\frac{\partial \theta_0}{\partial \eta}\right)^2 + 2u_0\frac{\partial \theta_0}{\partial \eta} + h(\phi_0-\theta_0)-\gamma_1\theta_1 + \\
&\quad jY_0^\alpha X_0^\beta(1+(e-2)\wp_0), \qquad \theta_1(\eta,0)=0, \qquad \theta_1(0,t)=0, \qquad \left.\frac{\partial \theta_1}{\partial \eta}\right|_{\eta=1}=0
\end{aligned}\right\} \tag{37}$$

$$\left.\begin{aligned}
\frac{\partial X_1}{\partial t} &= \frac{1}{Pem}\frac{\partial^2 X_1}{\partial \eta^2} + \frac{1}{Pem}\phi_0\frac{\partial^2 X_0}{\partial \eta^2} + \frac{1}{Pem}\frac{\partial \phi_0}{\partial \eta}\frac{\partial X_0}{\partial \eta} + 2u_0\frac{\partial X_0}{\partial \eta} + p\,Re\eta(1-\eta)\frac{\partial X_0}{\partial \eta} \\
&\quad + mY_0^\alpha X_0^\beta(1+(e-2)\wp_0), \qquad X_1(\eta,0)=0, \qquad X_1(0,t)=0, \qquad \left.\frac{\partial X_1}{\partial \eta}\right|_{\eta=1}=0
\end{aligned}\right\} \tag{38}$$

$$\frac{\partial Y_1}{\partial t} = 2u_0\frac{\partial Y_0}{\partial \eta} + \delta_3\left(\beta X_1 X_0^{\beta-1}Y_0^\alpha + \alpha Y_1 Y_0^{\alpha-1}X_0^\beta\right) \qquad Y_1(\eta,0)=0, \qquad Y_1(0,t)=0 \tag{39}$$

$$\frac{\partial u_1}{\partial t} = \frac{1}{Re}\frac{\partial^2 u_1}{\partial \eta^2} + \frac{1}{Re}\theta_0\frac{\partial^2 u_0}{\partial \eta^2} + \frac{1}{Re}\frac{\partial \theta_0}{\partial \eta}\frac{\partial u_0}{\partial \eta}, \qquad u_1(\eta,0)=0, \quad u_1(0,t)=0, \quad u_1(1,t)=0 \tag{40}$$

Using eigenfunctions expansion method and direct integration, we obtain the solution of equations (31) - (40) as:

$$u_0(\eta,t)=\frac{1}{\epsilon}(1-\eta)+\sum_{n=1}^{\infty} Me^{Nt}\sin n\pi\eta \tag{41}$$

$$\phi_0(\eta,t)=q+\sum_{n=1}^{\infty}\frac{A}{S}(1-e^{St})\sin\left(\frac{(2n-1)\pi\eta}{2}\right) \tag{42}$$

$$\theta_0(\eta,t)=q_2+\sum_{n=1}^{\infty}\frac{C}{B}(1-e^{Bt})\sin\left(\frac{(2n-1)\pi\eta}{2}\right) \tag{43}$$

$$X_0(\eta,t)=1 \tag{44}$$

$$Y_0(\eta,t)=1 \tag{45}$$

$$\phi_1(\eta,t)=\sum_{n=1}^{\infty}\left[\begin{array}{l}\dfrac{2q}{Pe}\left(\sum_{n=1}^{\infty}-\dfrac{AD^2}{8S^2}\left(2e^{St}-e^{2St}-1\right)\right)+\dfrac{4A_2}{D\pi}\left(\dfrac{e^{St}-1}{S}\right)\\[2mm]+\dfrac{2}{Pe}\sum_{n=1}^{\infty}\left(\sum_{n=1}^{\infty}-\dfrac{\pi A^2 D^2}{2S^3}\left(3e^{St}-3e^{2St}+e^{3St}-1\right)\right)\\[2mm]-\dfrac{4}{\in}\sum_{n=1}^{\infty}\dfrac{A}{4S^2}\left(2e^{St}-e^{2St}-1\right)+2f\sum_{n=1}^{\infty}\dfrac{A}{2S^2}\left(2e^{St}-e^{2St}-1\right)\\[2mm]+\dfrac{4}{\in}\sum_{n=1}^{\infty}\dfrac{A}{2S^2}\left(2e^{St}-e^{2St}-1\right)+2p\,Re\sum_{n=1}^{\infty}\dfrac{A}{2S^2}\left(2e^{St}-e^{2St}-1\right)\\[2mm]-2f\sum_{n=1}^{\infty}\dfrac{C}{2BS}\left(e^{St}+e^{Bt}-e^{(B+S)t}-1\right)\\[2mm]+2A_1\sum_{n=1}^{\infty}\dfrac{C}{2BS}\left(e^{St}+e^{Bt}-e^{(B+S)t}-1\right)\\[2mm]-2p\,Re\sum_{n=1}^{\infty}\dfrac{A}{4S^2}\left(\dfrac{\pi^2 D^2-4}{\pi^2 D^2}\right)\left(2e^{St}-e^{2St}-1\right)\\[2mm]+\dfrac{2}{pe}\sum_{n=1}^{\infty}\left(\sum_{n=1}^{\infty}-\dfrac{\pi DA^2}{3S^3}\left(3e^{St}-3e^{2St}+e^{3St}-1\right)\right)\end{array}\right]\sin\left(\dfrac{D}{2}\right)\pi\eta \qquad (46)$$

$$\theta_1(\eta,t)=\sum_{n=1}^{\infty}\left[\begin{array}{l}\dfrac{2q_2}{Pe}\sum_{n=1}^{\infty}-\dfrac{D^2 C\pi^2}{8B^2}\left(2e^{Bt}-e^{2Bt}-1\right)\\[2mm]+\dfrac{2}{Pe}\sum_{n=1}^{\infty}\left(\sum_{n=1}^{\infty}\dfrac{DC^2\pi}{3B^3}\left(3e^{Bt}-3e^{2Bt}+e^{3Bt}-1\right)\right)\\[2mm]+\dfrac{2}{Pe}\sum_{n=1}^{\infty}\left(\sum_{n=1}^{\infty}-\dfrac{D^2 C^2\pi^2}{6B^3}\left(3e^{Bt}-3e^{2Bt}+e^{3Bt}-1\right)\right)\\[2mm]+2h\sum_{n=1}^{\infty}\dfrac{A}{2BS}\left(e^{Bt}+e^{St}-e^{(B+s)t}-1\right)\\[2mm]+\dfrac{4}{\in}\sum_{n=1}^{\infty}\dfrac{\left(2e^{Bt}-e^{2Bt}-1\right)C}{2B^2}-\dfrac{4}{\in}\sum_{n=1}^{\infty}\dfrac{C\left(2e^{Bt}-e^{2Bt}-1\right)}{4B^2}\\[2mm]+2B_1\sum_{n=1}^{\infty}\dfrac{C}{2B^2}\left(2e^{Bt}-e^{2Bt}-1\right)\\[2mm]-2h\sum_{n=1}^{\infty}\dfrac{C}{2B^2}\left(2e^{Bt}-e^{2Bt}-1\right)+\dfrac{2B_2}{BD\pi}\left(e^{Bt}-1\right)\end{array}\right]\sin\left(\dfrac{D\pi\eta}{2}\right) \qquad (47)$$

$$X_1(\eta,t)=\sum_{n=1}^{\infty}\dfrac{4C_2\left(e^{Kt}-1\right)}{K\pi D}\sin\left(\dfrac{D}{2}\right)\pi\eta+\sum_{n=1}^{\infty}\left(2C_1\sum_{n=1}^{\infty}\dfrac{\left(e^{Kt}+e^{Bt}-e^{t(B+K)}-1\right)}{2BK}\sin\left(\dfrac{D}{2}\right)\pi\eta\right) \qquad (48)$$

$$Y_1(\eta, t) = \left| \begin{array}{l} \beta\delta_3 e^{-\alpha\delta_3 t} \sum_{n=1}^{\infty} \frac{4C_2}{K\pi D}\left(\frac{e^{t(K-\alpha\delta_3)}}{K-\alpha\delta_3} + \frac{e^{-\alpha\delta_3 t}}{\alpha\delta_3} \right)\sin\left(\frac{D}{2}\right)\pi\eta \\ + \beta\delta_3 e^{-\alpha\delta_3 t} \\ \sum_{n=1}^{\infty}\left(2C_1 \sum_{n=1}^{\infty} \frac{1}{2BK}\left(\frac{e^{t(K-\alpha\delta_3)}}{(K-\alpha\delta_3)} + \frac{e^{t(B-\alpha\delta_3)}}{(B-\alpha\delta_3)} - \frac{e^{t(B+K-\alpha\delta_3)}}{(B+K-\alpha\delta_3)} + \frac{e^{-\alpha\delta_3 t}}{\alpha\delta_3} \right)\sin\left(\frac{D}{2}\right)\pi\eta \right) \end{array} \right|$$

$$\begin{array}{l} -\beta\delta_3 e^{-\alpha\delta_3 t} \sum_{n=1}^{\infty} \frac{4C_2}{K\pi D}\left(\frac{1}{K-\alpha\delta_3} + \frac{1}{\alpha\delta_3} \right)\sin\left(\frac{D}{2}\right)\pi\eta - \beta\delta_3 e^{-\alpha\delta_3 t} \\ \sum_{n=1}^{\infty}\left(2C_1 \sum_{n=1}^{\infty} \frac{1}{2BK}\left(\frac{1}{(K-\alpha\delta_3)} + \frac{1}{(B-\alpha\delta_3)} - \frac{1}{(B+K-\alpha\delta_3)} + \frac{1}{\alpha\delta_3} \right)\sin\left(\frac{D}{2}\right)\pi\eta \right) \end{array} \right\} (49)$$

$$u_1(\eta, t) = \sum_{n=1}^{\infty} \left| \begin{array}{l} \frac{2e^{Nt}}{\in \text{Re}} \sum_{n=1}^{\infty} \frac{2Cn(2n-1)}{(4n-1)B}\left(1-e^{Bt}\right)\left(\frac{1-e^{-Nt}}{N}\right) - \\ \frac{2e^{Nt}}{\text{Re}} \sum_{n=1}^{\infty}\sum_{n=1}^{\infty}\left(\frac{\frac{CMn^2\pi e^{Nt}(1-e^{Bt})}{B}}{\left(\frac{1}{(4n+2)}+\frac{1}{(12n-2)}-\frac{1}{(2n-1)}\right)\left(\frac{1-e^{-Nt}}{N}\right)} \right) \\ -\frac{2e^{Nt}q_2}{\text{Re}} \sum_{n=1}^{\infty} \frac{\frac{Mn^2\pi^2 e^{Nt}}{2}\left(\frac{1-e^{-Nt}}{N}\right) -}{\frac{2e^{Nt}}{\text{Re}} \sum_{n=1}^{\infty}\left(\sum_{n=1}^{\infty} -\frac{Mn^2\pi e^{Nt}(-1)^n}{4B}\right)\left(\frac{1-e^{-Nt}}{N}\right)} \end{array} \right| \sin(n\pi\eta) \qquad (50)$$

where

$$M = \frac{2(1-(-1)^n)}{n\pi \in}, \quad N = -\frac{1}{\text{Re}}(n\pi)^2 \quad A_1 = -\frac{4\gamma(a-q)}{(2n-1)\pi}, \quad B = -\gamma - \frac{1}{pe}(n\pi)^2,$$

$$C = -\frac{2\gamma_1 a_1}{n\pi}, \quad A_1 = g(e-2), D = (2n-1), B_1 = j(e-2), C_1 = m(e-2), K = -\frac{1}{pem}\left(\frac{(2n-1)\pi}{2}\right)^2,$$

$$A_2 = fq - fq_2 + g + q_2 g(e-2), B_2 = hq + j + q_2 j(e-2) - q_2 h, C_2 = m + mq_2(e-2),$$

The computations were done using computer symbolic algebraic package MAPLE (version 17, Maplesoft, USA)

Results and Discussion

The system of partial differential equations describing the transient in-situ combustion of oil shale in porous medium has been solved analytically using eigenfunctions expansion method and direct integration. The analytical solutions (equations (41) - (50)) are computed and presented graphically with the aid of computer symbolic algebraic package MAPLE 17 for various values of dimensionless parameters, $\delta_0, \delta_1, \sigma_0$ and σ_1.

Figure1 presents the influence of Frank-Kamenetskii number δ_0 on gas phase temperature profile. It is observed that gas phase temperature increases significantly along distance as Frank-Kamenetskii number increases. This is due to increase in heat of reaction ΔH.
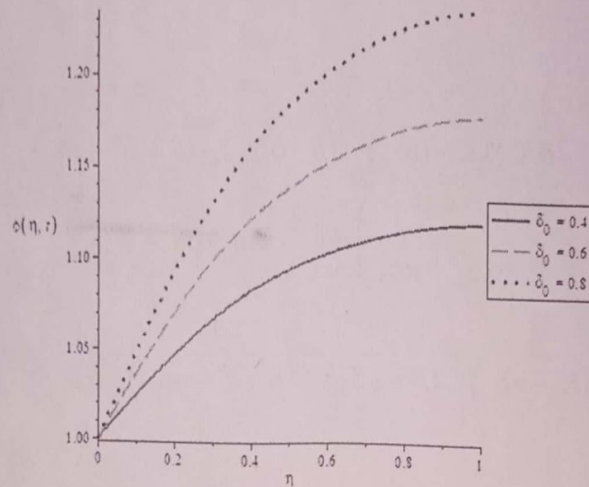

Figure 1: Gas phase temperature $\phi(\eta,t)$ against distance η for different values of δ_0 and

$$P_{em} = 1,\ p_e = 1,\ R_e = 1,\ \delta = 0.4,\ \sigma = 0.01, D_a = 1,\ \epsilon = 0.01, \alpha = 1, \beta = 1, q = 1,\ q_2 = 0.01\ \gamma = 1$$

Figure 2 displays the effect of Frank-Kamenetskii number δ_0 on gas phase temperature profile. It is observed that gas phase temperature increases significantly with time as Frank-Kamenetskii number increases.
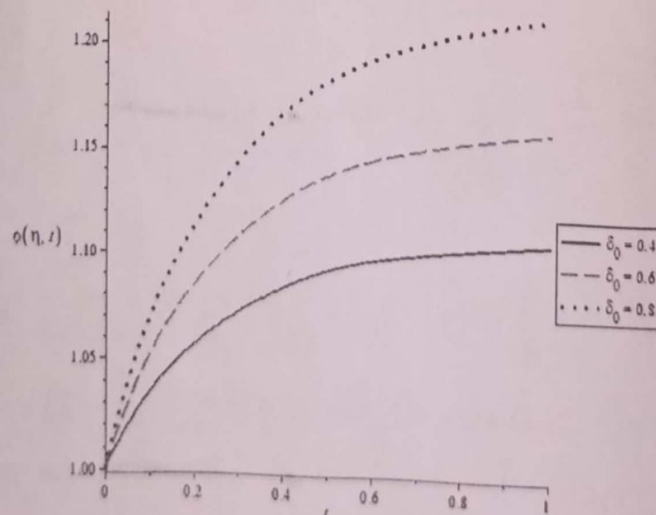

Figure 2: Gas phase temperature $\phi(\eta,t)$ against time t for different values of δ_0 and

$$P_{em} = 1,\ p_e = 2,\ R_e = 1,\ \delta = 0.4, \sigma = 0.01,\ D_a = 1,\ \epsilon = 0.01, \alpha = 1, \beta = 1, q = 1,\ q_2 = 0.01\ \gamma = 1$$

Figure 3 shows the effect of Frank – Kamenetskii number δ_1 on solid phase temperature profile. It is observed that solid phase temperature increases significantly along distance as Frank-Kamenetskii number increases. This is due to increase in heat of reaction
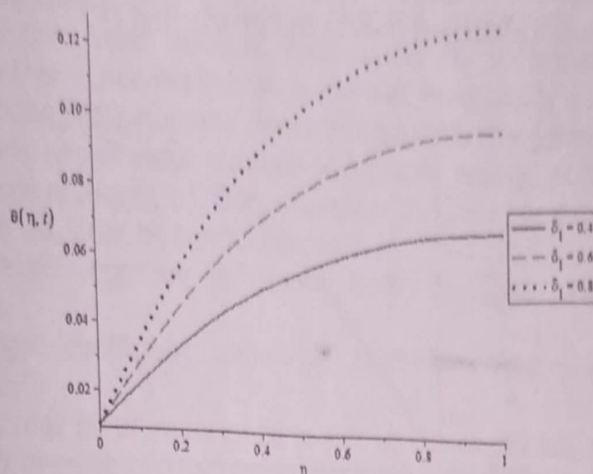
Figure 3: Solid phase temperature $\theta(\eta, t)$ against distance η for different values of δ_1 and

$$P_{em} = 1, \; p_e = 1, \; R_e = 1, \; \delta = 0.4, \; \sigma = 0.01, D_a = 1, \; \epsilon = 0.01, \alpha = 1, \beta = 1, q = 1, q_2 = 0.01, \; \gamma = 1$$

Frank-Kamenetskii number increases. Clearly, Frank-Kamenetskii number improves production of gas due to increase in heat of reaction. When there is increase in heat of reaction the gas production rate is boosted.
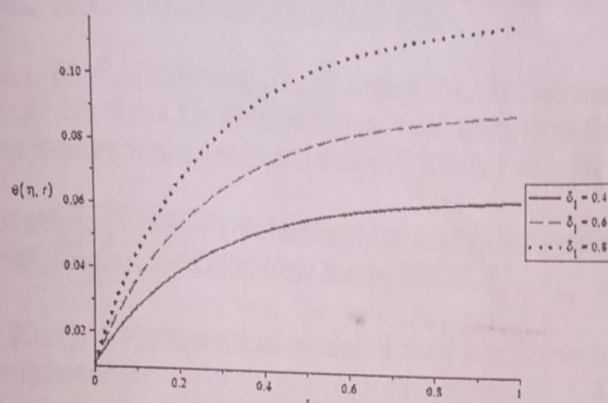

Figure 4: solid phase temperature $\theta(\eta, t)$ against time t for different values of δ_1 and

$$P_{em} = 1, \; p_e = 2, \; R_e = 1, \; \delta = 0.4, \sigma = 0.01, D_a = 1, \; \epsilon = 0.01, \alpha = 1, \beta = 1, q = 1, q_2 = 0.01, \; \gamma = 1$$

Figure 5 depicts the effect of σ_0 on gas phase temperature profile. It is observed that gas phase temperature increases with time (t) as σ_0 increases.
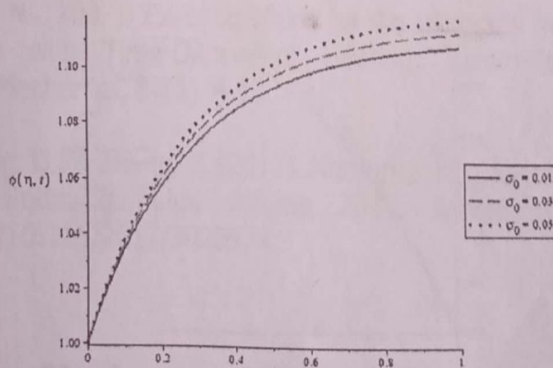

Figure 5: Gas phase temperature $\phi(\eta, t)$ against time t for different values of σ_0 and

$$P_{em} = 1, \; p_e = 2, \; R_e = 1, \; \delta = 0.4, \sigma = 0.01, D_a = 1, \; \epsilon = 0.01, \alpha = 1, \beta = 1, q = 1, q_2 = 0.01, \; \gamma = 1$$

Figure 6 displays the effect of σ_1 on gas phase temperature profile. It is observed that gas phase temperature increases significantly along distance as Heat exchange coefficient increases. Obviously, Heat exchange coefficient boosts the production of
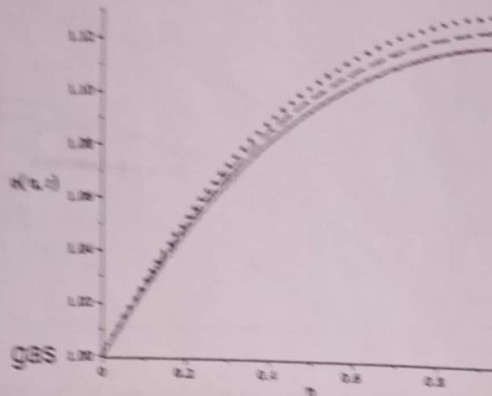

Figure 6: Gas phase temperature $\phi(\eta, t)$ against distance η for different values of σ_1 and $P_m = 1, p_e = 2, R_e = 1, \delta = 0.4, \sigma = 0.01, D_e = 1, \epsilon = 0.01, \alpha = 1, \beta = 1, q = 1, q_1 = 0.01, \gamma =$

Figure 7 represents the effect of σ_1 on solid phase temperature profile. It is observed that solid phase temperature increases with time (t) as σ_1 increases.
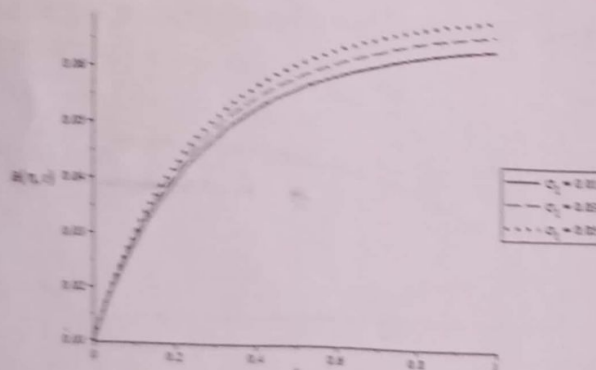

Figure 7: Solid phase temperature $\theta(\eta, t)$ against time: for different values of σ_1 and $P_m = 1, p_e = 2, R_e = 1, \delta = 0.4, \sigma = 0.01, D_e = 1, \epsilon = 0.01, \alpha = 1, \beta = 1, q = 1, q_1 = 0.01, \gamma = 1$

Figure 8 displays the effect of σ_1 on solid phase temperature profile. It is observed that solid phase temperature increases significantly along distance as Heat exchange coefficient increases
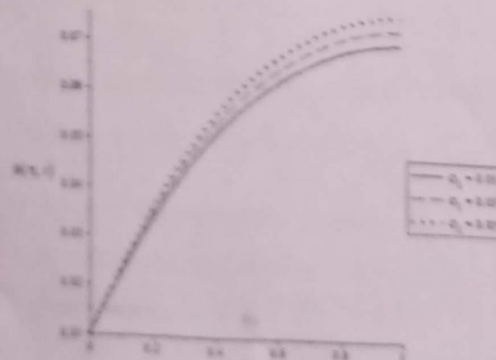

Figure 8: Gas phase temperature $\phi(\eta, t)$ against distance η for different values of σ_1 and $P_m = 1, p_e = 2, R_e = 1, \delta_1 = 0.4, \sigma = 0.01, D_e = 1, \epsilon = 0.01, \alpha = 1, \beta = 1, q = 1, q_1 = 0.01, \gamma = 1$

Conclusion

In this study, a one-dimensional transient coupled mass and heat transport model incorporating combustion front velocity, formulated to determine the distribution of temperature and species concentration in a porous medium is solved analytically using eigenfunctions expansion technique and direct integration. The governing parameters of the problem are the Frank-Kamenetskii number (δ), Peclet energy number (P_e), Peclet mass number, (P_{em}), Reynolds number (R_e), Darcy number (D_a), and Heat exchange coefficient. (σ) From the results obtained, it can be concluded that:

(i) Frank-Kamenetskii number enhanced both the gas phase and solid phase temperatures.

(ii) Heat exchange coefficient enhanced both the gas phase and solid phase temperatures.

(iii) These results may be of importance to petroleum engineers, geologists and scholars attempting to develop programming standards and to researchers interested in the theoretical aspects of oil shale combustion.

References

Ayeni, R. O. (1978). Thermal runaway. Unpublished PhD Thesis, Cornell University, USA.

Abdelrahman, A. A. (2015). Geological overview of oil shale https:// www.researchgate.net//publication/282354048.

Lapene, A., Martins, M. F., Debenest, G., Quintard, M., & Salvador, S. (2007). Numerical Simulation of Oil Shale Combustion in a Fixed bed: Modeling and Chemical Aspect. https//www.researchgate.net/publication/27333515. Alb, France.

Myint-U, T., & Debnath, L. (1987). Partial differential equation for scientist and engineers. PTR Prentice- Hall, Englewood Cliffs. New Jersey 07632.

Olayiwola, R. O. (2011). A Mathematical model of solid fuel arrhenius combustion in a fixed —bed. *International Journal of Numerical Mathematics*, 6(2), 214-233.

Olayiwola R. O. (2011). A Mathematical model of in-situ combustion as enhanced oil recovery technique in Porous Media. Unpublished PhD Thesis, Lautech Ogbomoso, Nigeria.

Olayiwola, R. O. (2012). Fixed – bed solid fuel Arrhenius combustion: Modeling and simulation. *Journal of the Nigeria of Mathematical Physics*, 21, 111-120.

Toki, C. J. & Tokis, J. N. (2007). Exact solutions for the unsteady free convection flows on a porous plate with Time-Dependent Heating. Zamm-Zeitchrift for Angewadte Mathematics Mechanics, 87(1) ,4-13.

Zheng, H., Shi, W., Dig, D., & Zhang, C. (2017) .Numerical simulation of In-situ combustion of oil Shale. HindawGeofluids Volume 2017, Article ID 3028974, 9 pages. Http//doi.org/10.115/2017/3028974.